MODELING AND VERIFICATION OF

NATURALISTIC LANE KEEPING SYSTEM

A Thesis

by

ZHEREN ZHOU

Submitted to the Office of Graduate and Professional Studies of
Texas A&M University
in partial fulfillment of the requirements for the degree of

MASTER OF SCIENCE

Chair of Committee,	Reza Langari
Committee Members,	Swaroop Darbha
	Wei Zhan
Head of Department,	Andreas A. Polycarpou

August 2016

Major Subject: Mechanical Engineering

ABSTRACT

In order to lower human drivers' driving load and to enhance their systematic performance during driving, driver assistant systems have been introduced during the past few decades. Unfortunately, a large proportion of existing lane keeping techniques only focus on how to hold the car in the center of the lane, which may be contrary to the driver's natural motion sense. This research focuses on developing a rational and precise driver model with fully human driver operating behavior, which is crucial for the study of active safety technology and can provide drivers with a comfortable motion by imitating driving habits and trajectory.

Modeling a naturalistic lane keeping control requires understanding of how a driver operates the vehicle, analysis from vehicle lateral dynamics perspective, and knowledge of the combination of driver's physical limitation. Another requirement to build an adaptive steering control model is to regard driver's steering behavior as a reciprocal process between anticipation and compensation. Based on two angles (near and far angles) mechanism and experimental data recorded by the SIMULINK and dSpace co-platform, a close-loop system is designed. The whole system is a combination of a PI (proportional–integral) controller driver model and a vehicle model, which integrates vehicle lateral dynamic characteristics and upcoming road information. Moreover, a nonlinear steering driver model is designed. This open loop driver model can effectively correct steering wheel angle by minimizing the error between recorded driving data and that of the simulated model.

The simulation outcome shows that the proposed model captures human drivers'

behavior well and has an excellent adaptability towards the change of vehicle dynamic parameters and external disturbances.

NOMENCLATURE

LKS	Lane-Keeping System
LKA	Lane Keeping Aid
LDW	Lane Departure Warning
CG	Center of Gravity
MP	Momentary Pole
PI	Proportional Integral
LAD	Least Absolute Deviations
LAE	Least Absolute Errors
SIT	System Identification Toolbox

TABLE OF CONTENTS

Page

ABSTRACT ii

NOMENCLATURE iv

TABLE OF CONTENTS v

LIST OF FIGURES vii

LIST OF TABLES ix

CHAPTER I INTRODUCTION 1

1.1 Research background and significances 1
1.2 Related work 4
1.3 Thesis objectives 8
1.4 Thesis outline 9

CHAPTER II VEHICLE MODEL AND ROAD REFERENCE SYSTEM 11

2.1 Vehicle dynamic model 12
2.2 Driver's visual attention mechanism research 17
2.3 Road reference system 19
2.4 Simulation experiment design 22

CHAPTER III ANALYSIS OF DRIVER BEHAVIOR 25

3.1 Driving strategy 27
3.2 Analysis of steering 30
3.3 Calculation of two angles 33

CHAPTER IV SIMULATION AND RESULTS 35

4.1 PI controller identification 36
4.2 Modelling by system identification toolbox 42

CHAPTER V CONCLUSION AND OUTLOOK 46

5.1 Conclusion 46

5.2 Outlook 46

REFERENCES 48

LIST OF FIGURES

FIGURE Page

1.1 The Ratio of Crashes Caused by Drowsy Driving [1] 1

1.2 Distraction Detection Scheme [3] 2

1.3 Comparison of Two Lane Keeping Systems 3

1.4 Shaft Driver Model [4] 5

1.5 A Structural Scheme of Human Steering Behavior in the Driver-Vehicle-Road System [5] 6

2.1 Vehicle Model with Four Wheels Steering [12] 12

2.2 Single Track Model Equivalent Diagram [12] 12

2.3 Kinematic Variables [12] 14

2.4 Vehicle Heading and Lateral Offset [12] 16

2.5 Driver Steering Fixation Area 18

2.6 Two Points (Near and Far) Mechanism 18

2.7 The Geometric Relationship between Vehicle and Upcoming Road 20

2.8 Screenshot of DSpace 22

2.9 Test Track in DSpace 24

3.1 Test Track Details 25

3.2 Data Recorded in DSpace 26

3.3 Recorded Track 27

3.4 Straight Lane Comparison 28

3.5 The Racing Line [23] 29

3.6 Bend Comparison 29

3.7 Steering Angle of Three Drivers 31

3.8 JMP Example 31
3.9 Far Distance 33
3.10 Far and Near Angle 34
4.1 Modeling Approaches [29] 35
4.2 System Structure using PI Controller 37
4.3 Near Angle Comparison 38
4.4 Far Angle Comparison 38
4.5 Lateral Offset Comparison 40
4.6 Three Steps 41
4.7 Comparison of Path on Taking Curve Step 41
4.8 SIT Data Processing Flow [29] 42
4.9 SIT Identification Mechanism [29] 43
4.10 Nonlinear ARX Identification [29] 44
4.11 Steering Angle Comparison 44

LIST OF TABLES

TABLE Page

2.1 Main Parameters of Vehicle Model 13

2.2 Vehicle Model Parameters in DSpace 23

3.1 Selected Data 27

3.2 Comparison of Steering Angle 32

3.3 Data Processing Example in EXCEL 33

4.1 Match Percentage of Identification Model 39

CHAPTER I

INTRODUCTION

1.1 Research Background and Significances

A recent survey states out that among traffic accidents, about 21% relate to driver fatigue [1], especially when driving on a highway because the extended period of driving leads to driver fatigue and distraction. Driver's physical or psychological fatigue is one of the factors that lead to the frequent occurrence of traffic accidents. Another fact that could induce traffic accidents is lack of proficient driving experience, which is sometimes due to age (very high or very low).

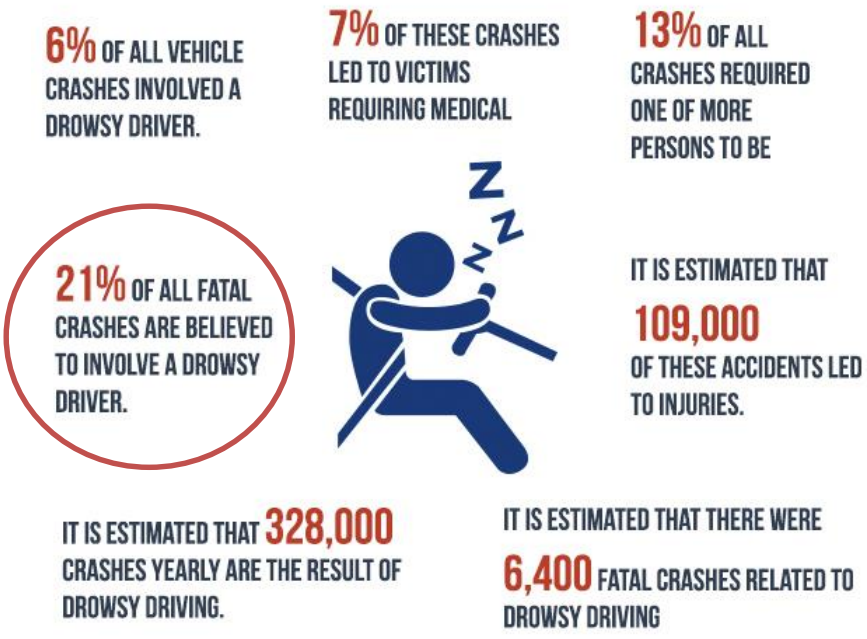

Figure 1.1: The Ratio of Crashes Caused by Drowsy Driving [1]

In order to lower human drivers' driving load and to enhance their systematic performance during driving, driver assistance systems have been introduced during the past few decades. These driver assistant systems comprise lane departure warning system,

parking assist system, advanced collision warning system and self-adaptive cruise control. Autonomous driving systems expand on these and include lane keeping system and obstacle avoidance system. These vehicle active safety technologies can alleviate driver's operating load and forecast latent danger in advance. Besides, the technology can even replace human drivers' operation to prevent and reduce the traffic accidents.

For instance [2], 2016 Ford Fusion uses the Lane Keeping System (LKS), which both includes functions of Lane Keeping Aid (LKA) and Lane Departure Warning (LDW). A camera, which is mounted behind the windscreen, can determine the vehicle position and detect lane departure happening by watching the lane marking as depicted in Figure 1.2 [3]. Lane keeping alert warns the driver by a series of vibrations of the steering wheel. On the other hand, Lane keeping system (LKS) will take action automatically after warning to ensure the vehicle stays within road boundaries.

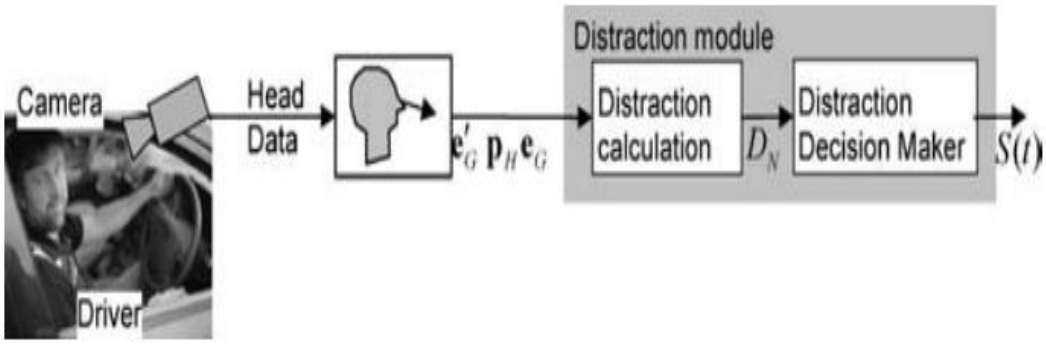

Figure 1.2: Distraction Detection Scheme [3]

Unfortunately, a large proportion of existing lane keeping techniques only focus on how to hold the car in the center of the lane, which may be contrary to the driver's natural motion sense. As Figure 1.3 shown, the experienced driver typically chooses to cut

the curve to shorten the passing time. While a less experienced driver may take a longer distance around the curve. On the other hand, studies in this field typically focuses on low speed and large radius curvature conditions, which prevent their generalization to other common situation in highway driving. Thus, a reasonable and naturalistic diver-vehicle-road close-loop model is needed to make up for the lack of research in this area.

Figure 1.3: Comparison of Two Lane Keeping Systems

To satisfy the above requirement, this research focuses on developing a rational and precise driver model with fully human driver operating behavior, which is crucial for the study of active safety technology and can provide drivers with a comfortable motion by imitating driving habits and trajectories. Moreover, the Naturalistic Lane-Keeping System has a promising market, practical significance and application like training and teaching inexperienced drivers, or replacing human test driver in experiments to reduce personal injury.

1.2 Related Work

How do drivers steer their car rounds curves of a winding road? On the face of it, this would seem to be a simple task that can be achieved effortlessly by steering approaching the center to correct the lateral error using the real-time position of the car on the road. Nevertheless, on account of the fact that the driver's attention can be diverted from the steering task for extended periods of time and inherent delays between action and perception, this low-level error correction strategy is not sufficient in high-speed conditions. In the research on human drivers' behavioral habit, researchers combine the characteristics of the driver model with that of physiology and psychology. Besides, driver model bears the following features: (1) Driver model grasps human driver's controlling skills and traits, like the ability of (visual, haptic, hearing) information reception, prediction, decision making, neuromuscular dynamics, operation restriction, learning ability, time-lag, memory, and so on; (2) Drivers of different experience and age have diverse driving styles; (3) Driver model should be provided with properties of concentration, fatigue, tension, and other emotional features. Only a model possesses one or more than one characteristic mentioned above, can be called a real driver model.

According to the principles aforementioned, this section lists several representative driver models. At the early stage of driver model research, researchers regarded it as driver's operation toward the vehicle, which could be modeled by mathematical expressions. Based on classical control theory, researchers deemed driver model as a time-lagging transfer function.

In 1953, Kondo [4] established the first driver model using one point preview

method, called “Shaft” as depicted in Figure 1.4.

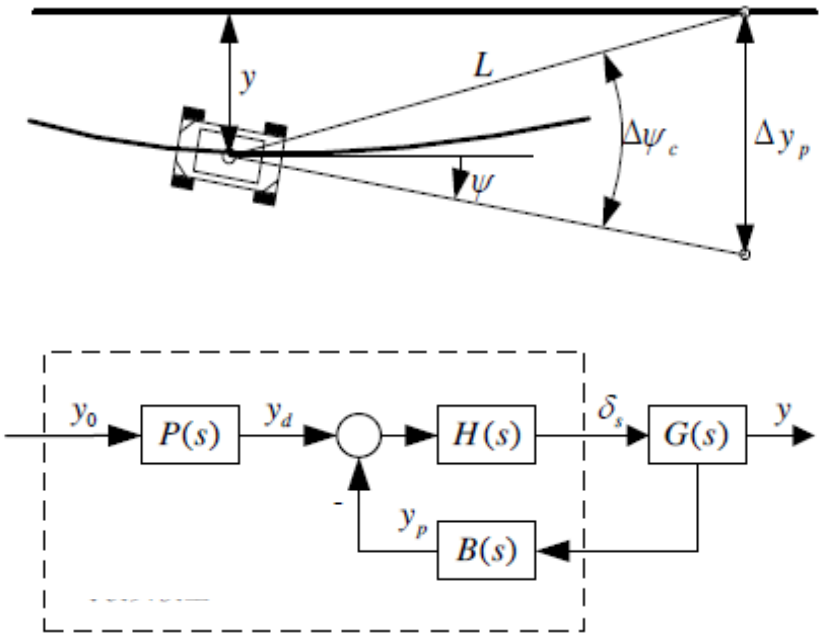

Figure 1.4: Shaft Driver Model [4]

The author estimated the lateral distance based on the current vehicle position and the preview time, then made the lateral distance gradually reduce to zero gradually to ensure the car moves in the desired trajectory.

Donges [5] proposed an improved two-level model which is composed of both closed-loop compensatory control and open-loop anticipatory control to produce successful navigation: the compensation of lateral position errors utilize the immediate information from the near region helps to adjust the car current location; the measurements include road curvature error and lateral distance error. Meanwhile, through the observation of the road at a distance, far region information contributes to preview the future trajectory for anticipatory control. This is depicted in Figure 1.5.

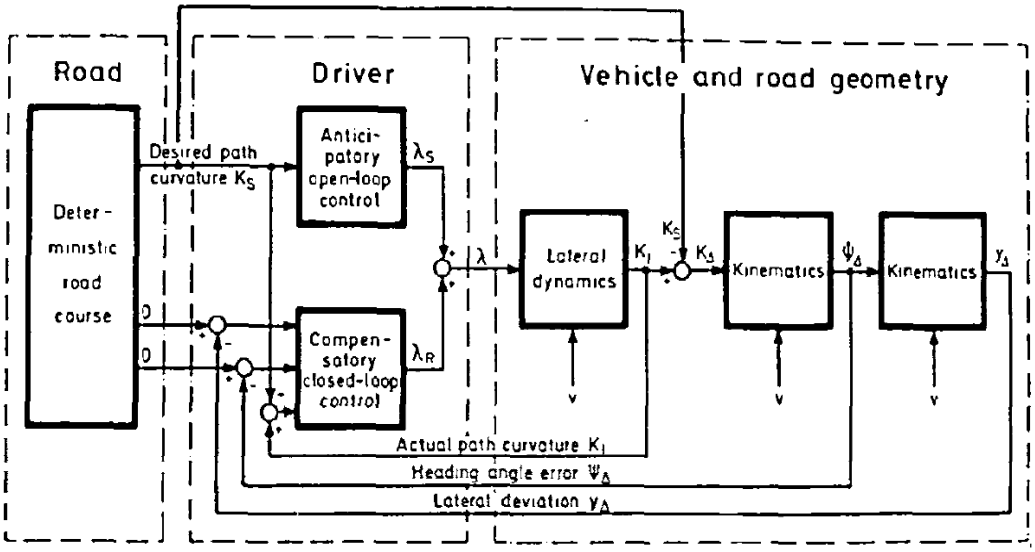

Figure 1.5: A Structural Scheme of Human Steering Behavior in the Driver-Vehicle-Road System [5]

As modern control theory was growing and maturing in the end of 1980s', researchers tried to use artificial intelligence to establish driver model. Representative technologies include Fuzzy Logic and Neural network Algorithm. Zeyada [6] proposed a fuzzy logic control device, which took steering and braking into consideration and could be used to track path and avoid collisions. Differentiated from Hessburg's [7] fuzzy logic controller, Zeyada's controller input information was collected from vehicle's distance from the left, the right, right ahead, front-left, front-right, and other multiple directions. This controller could control the vehicle's steering operation and vertical operation separately by using two parallel fuzzy logic controllers. By previewing the distance information from every direction, the controller can decide the size and direction of the steering angle.

Because of its excellent ability of approximation, ability neural networks were

used to imitate the human driver's behavior since 1990s [8]. Kraiss [9] presented a neural network driver model that would be used in a driver assistance system where the model's input parameters were vehicle's lateral distance from nearby paths, vehicle lateral location, and velocity. In 2004, the first two-point model paper was published [10], in which a proportional integral and a proportional controllers were utilized individually for anticipation and compensatory based on the two angle mechanism. This article provided a comparison of real drivers' strategy using the proposed model on three different studies: curve negotiation, corrective steering and lane changing. Based on the experiment data, the author validated that this driver model can be the explanation for how humans control the moving path. Nonetheless, it is not realistic to assume human driver consistently holds the vehicle in the centerline of the road. Consequently, the assessment is just a rough guesstimate for the human driving habit in true life.

To demonstrate the two point mechanism is convincing, another researcher compares two type of guiding control method including two angle method and one point method [11]. Analyzing the data obtained by their driving simulation lab, the conclusion comes out with using two points method to predict steering wheel angle can match the experimental data and the result is more accurate than using the one-point navigating approach to estimate the path of vehicle.

To sum up, the above models establish the driver model based on classical modern control theory including non-conventional method such as fuzzy logic and neural networks have merits and demerits respectively.

1.3 Thesis Objectives

The rationale for driver model is that it can be used to evaluate the stability of vehicle operation. At the beginning period of researching driver model, many researchers focus on driver-vehicle closed-loop system from a control theory perspective. Such perspective regards divers and vehicles as a time-lagged mathematical model that compensates for the vehicle according to vehicle status feedback. Large amounts of early literature regard driver-vehicle system as a regular mechanical systems does not include the analysis and evaluation of the driver's characteristics (like driving skill or driving experience, etc.) These method ignore the fact that the driver has his/her own preview characteristics, which means the driver has the ability to perceive the driving circumstances in advance and adapt this decision accordingly. In other words, human driver can reasonably decide the driving direction, vertical or horizontal, in accordance with the known driving circumstance. Moreover, human driver's controlling behavior should be compatible with his/her own ability, be safe, comfortable, and stable. In more recent time, researchers deem that vehicle's characteristics should be reflected through driver's real operations towards the vehicle. Therefore, establishing a driver model that bears human driver's characteristics enables driver-vehicle closed-loop system to become closer to authentic driving situation and makes the evaluation of vehicle's stability comprehensive and reasonable. Establishing a driver model that possesses human driver's characteristics is also needed in automobile active safety research. Since the ultimate purpose of studying the automobile active safety technology is to partially or completely replace real human driver's operation, the consistency of characteristics of designed

system can lead to driver with a safer and more comfortable driving experience. For instance, the perception of driving circumstances (like highway curvature and obstacles) and the vehicle location is needed during path tracking process to enable reasonable direction control.

1.4 Thesis Outline

The first chapter is an introduction, which states the necessity and importance of the work by introducing the research background of intelligent vehicle's assist driving system.

The following chapter introduces a vehicle model that can be applied to naturalistic lane keeping system. At first, the chapter states the two points steering method. Then the vehicle motion formulation which comes from a series of geometric deductions, algebraic operations, and linearization is described.

The third chapter focuses on experimental environment design and implement including establishing the combined platform of SIMULINK and dSpace, plotting the test track in a software environment that meets the criterion of United State highway construction. In addition, analyzing the work of three subjects' driving behavior is done in this section to get ready for next step of diver controller design.

Next chapter is about the driver model design and integrated system identification and validation. PI controller and ARX nonlinear controller are presented in this chapter.

The final chapter lists the conclusions and expectations that systematically

present the work and outcomes of the thesis and discuss the future research directions and solutions for unsolved issues.

CHAPTER II

VEHICLE MODEL AND ROAD REFERENCE SYSTEM

This chapter presents the vehicle model via state space equations. We also present modified measurement equations for calculating the near and far points referring to road curvature. In straight path situations, the linearized approximation is commonly applied to achieve the near angle. However, this assumption fails in curved conditions. The curvature of the road must be taken into consideration to figure out the issue of far point. In realistic environments, the far angle can be captured for using computer vision techniques using an appropriately mounted camera. As one of the prerequisites, all vehicle parameters which will be used in later calculations are listed; at the same time, the methods about how to estimate tire cornering stiffness is introduced.

The track model used for driving test and collecting authentic human driving behavior data is also shown in this section. Subsequently, the last part of this chapter presents the experimental results of three different human driver's wheel trochoid and the comparisons between measured tracks with original test track.

2.1 Vehicle Dynamic Model

The "single track model" proposed by Schunck and Riekert [12] is widely used in the horizontal plane because it covers most essential features of car steering. The two front wheels are considered as a whole in the center line of vehicle, and the two rear wheels are assumed as one in the same way. Based on this assumption, the car model of Figure 2.1 can be reduced to that of Figure 2.2.

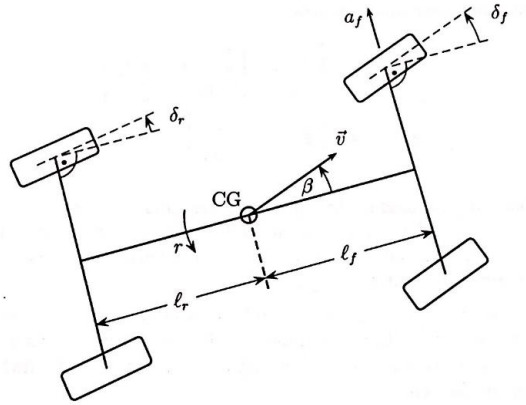

Figure 2.1: Vehicle Model with Four Wheels Steering [12]

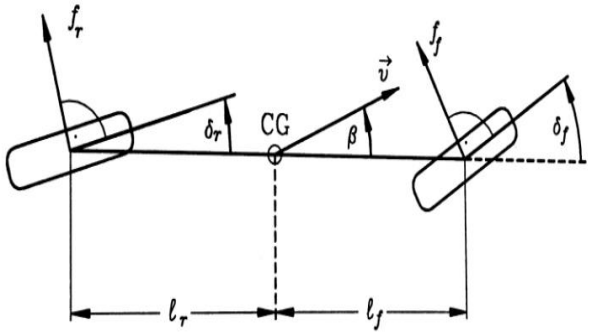

Figure 2.2: Single Track Model Equivalent Diagram [12]

The left figure 2.2 also shows a coordinate system (x_0, y_0) which is inertially fixed, and "yaw angle" φ is defined as the rotated angle of the vehicle coordinate system (x, y) like left figure shown. Road surface transmit side forces f_f *and* f_r via the wheels to

the car chassis. We assume the wheels can spin liberally. Braking and the acceleration by the engine are not taken into account on this model.

The physical meaning of the main parameters are shown on table 2.1.

Table 2.1 Main Parameters of Vehicle Model

Symbol	Implication	Symbol	Implication
CG	Center of gravity	l	Wheel base
l_f	Front wheel base	l_r	Rear wheel base
δ_f	Front steering angle	δ_r	Rear steering angle
α_r	Rear sideslip angle	α_f	Front sideslip angle
β	sideslip angle	φ	Yaw angle
γ	Yaw rate	v	Velocity
y_l	Lateral offset	J	Moment of Inertia
D_n	Near distance	D_f	Far distance
C_f	Front tire stiffness	C_n	Rear tire stiffness

Through the steering angles, the side forces f_f and f_r are projected onto the vehicle coordinates system (x, y). Thus, around the z axis, we have:

$$\begin{bmatrix} f_x \\ f_y \\ m_z \end{bmatrix} = \begin{bmatrix} -sin\delta_f & -sin\delta_r \\ cos\delta_f & cos\delta_r \\ l_f cos\delta_f & -l_r cos\delta_r \end{bmatrix} \begin{bmatrix} f_f \\ f_r \end{bmatrix} \quad (1)$$

From the geometric relationship in Figure 2.2, in the horizontal plane, the equations of motions:

a) Longitudinal:

$$-\mathrm{mv}\left(\dot{\beta}+\dot{\varphi}\right)sin\beta+m\dot{v}cos\beta=f_x \tag{2}$$

b) Lateral:

$$\mathrm{mv}\left(\dot{\beta}+\dot{\varphi}\right)cos\beta+m\dot{v}sin\beta=f_y \tag{3}$$

c) Yaw:

$$\mathrm{J}\ddot{\varphi}=m_z \tag{4}$$

With $\gamma=\dot{\varphi}$, we can get the matrix from of these equations:

$$\begin{bmatrix}\mathrm{mv}(\dot{\beta}+\dot{\gamma})\\ \mathrm{m}\dot{v}\\ \mathrm{J}\dot{\gamma}\end{bmatrix}=\begin{bmatrix}-\sin\beta & \cos\beta & 0\\ \cos\beta & \sin\beta & 0\\ 0 & 0 & 1\end{bmatrix}\begin{bmatrix}\mathrm{f_x}\\ \mathrm{f_y}\\ \mathrm{m_z}\end{bmatrix} \tag{5}$$

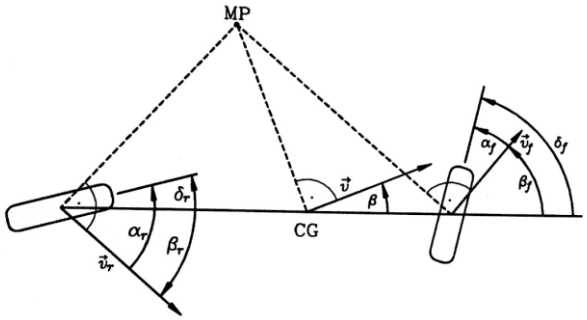

Figure 2.3: Kinematic Variables [12]

Figure2.3 depicts the geometric relationship between some related parameters such as velocity vectors of front and rear wheel. In addition, MP is defined as momentary pole.

In the longitudinal direction, the velocity components should equal to each other:

$$v_r cos\ \beta_r=v_f cos\beta_f=vcos\beta \tag{6}$$

The velocity elements vertical to the center line can be expressed using the yaw rate γ as:

$$v_f sin\beta_f = vsin\,\beta + l_f\,\gamma \tag{7}$$

$$v_r sin\,\beta_r = vsin\,\beta - l_r\,\gamma \tag{8}$$

After a division operation by the corresponding terms from Equation (6).The rear and front velocity v_r and v_f are eliminated. Hence, the following two equations can be obtained:

$$\tan\beta_f = \frac{v\sin\beta + l_f r}{v\cos\beta} = \tan\beta + \frac{l_f r}{v\cos\beta}$$

$$\tan\beta_r = \frac{v\sin\beta - l_r r}{v\cos\beta} = \tan\beta - \frac{l_r r}{v\cos\beta} \tag{9}$$

The tire sideslip angles are:

$$\alpha_f = \delta_f - \beta_f$$

$$\alpha_r = \delta_r - \beta_r \tag{10}$$

Then linearize the single-track model, we assume the sideslip angle β is small. Then matric (5) becomes:

$$\begin{bmatrix} mv(\dot{\beta} + r) \\ m\dot{v} \\ J\dot{\gamma} \end{bmatrix} = \begin{bmatrix} -\beta & 1 & 0 \\ 1 & \beta & 0 \\ 0 & 0 & 1 \end{bmatrix} \begin{bmatrix} f_x \\ f_y \\ m_z \end{bmatrix} \tag{11}$$

When $\dot{v}$ equals to 0 , chassis sideslip angle β_f, β_r and steering angle δ_f , δ_r are also assumed small, then

$$\begin{bmatrix} mv(\dot{\beta} + r) \\ J\dot{\gamma} \end{bmatrix} = \begin{bmatrix} f_y \\ m_z \end{bmatrix} \tag{12}$$

$$\begin{bmatrix} f_y \\ m_z \end{bmatrix} = \begin{bmatrix} 1 & 1 \\ l_f & -l_r \end{bmatrix} \begin{bmatrix} f_f(\alpha_f) \\ f_r(\alpha_r) \end{bmatrix} \tag{13}$$

$$\beta_f = \beta + \frac{l_f r}{v} \quad \beta_r = \beta - l_r r/v \tag{14}$$

$$f_f(\alpha_f) = c_f \alpha_f, \tag{15}$$

$$\alpha_f = \delta_f - \beta_f \tag{16}$$

$$f_r(\alpha_r) = c_r\alpha_r, \qquad (17) \qquad \alpha_r = \delta_r - \beta_r \qquad (18)$$

The linearized plant model follows from (12) to (15) as:

$$\begin{bmatrix} mv(\dot{\beta} + r) \\ J\dot{r} \end{bmatrix} = \begin{bmatrix} 1 & 1 \\ l_f & -l_r \end{bmatrix} \begin{bmatrix} c_f(\delta_f - \beta - l_f r/v) \\ c_r(\delta_r - \beta + l_r r/v) \end{bmatrix} \qquad (19)$$

Solving (16) for $\dot{r}$ and $\dot{\beta}$ to get the state-space equation matrix as:

$$\begin{bmatrix} \dot{\beta} \\ \dot{r} \end{bmatrix} = \begin{bmatrix} a_{11} & a_{12} \\ a_{21} & a_{22} \end{bmatrix} \begin{bmatrix} \beta \\ r \end{bmatrix} + \begin{bmatrix} b_{11} & b_{12} \\ b_{21} & b_{22} \end{bmatrix} \begin{bmatrix} \delta_f \\ \delta_r \end{bmatrix} \qquad (20)$$

$$a_{11} = -(c_r + c_f)/mv \qquad a_{12} = -1 + \frac{c_r l_r - c_f l_f}{mv^2}$$

$$a_{21} = (c_r l_r - c_f l_f)/J \qquad a_{21} = \frac{c_r l_r - c_f l_f}{J}$$

$$a_{22} = -(c_r l_r^2 + c_f l_f^2)/Jv \qquad b_{11} = \frac{c_f}{mv}$$

$$b_{12} = c_r/mv \qquad b_{21} = c_f l_f/J \qquad b_{22} = -c_r l_r/J$$

To conduct research of car steering mechanism, the vehicle model need to be enlarged. The lateral offset between the CG of vehicle and the centerline of the road, velocities as well as upcoming road curvature should also be taken into consideration to extend the steering model.

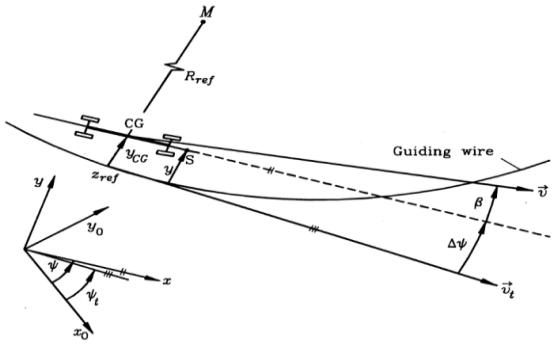

Figure 2.4: Vehicle Heading and Lateral Offset [12]

In the extended vehicle model, we consider ρ_{ref}=1/R_{ref} that is the upcoming

road curvature as the disturbance to produce the guide line. The difference angle between the tangent line and the centerline of the car can be presented as $\Delta\varphi = \varphi - \varphi_t$.

With the linearization $\sin(\beta + \Delta\varphi) \approx \beta + \Delta\varphi$, the lateral offset y is:

$$\dot{y} = v(\beta + \Delta\varphi) + l_n r \tag{21}$$

With the linearization $\sin(\beta + \Delta\varphi) \approx \beta + \Delta\varphi$, the lateral offset y is:

$$\Delta\dot{\varphi} = \dot{\varphi} - \dot{\varphi}_t = r - v\rho_{ref} \tag{22}$$

Combining (17), (18) and (19), and assuming the rear steering angle as zero, the integrated state-space model can be achieved as:

$$\begin{bmatrix} \dot{\beta} \\ \dot{r} \\ \Delta\dot{\varphi} \\ \dot{y} \end{bmatrix} = \begin{bmatrix} a_{11} & a_{12} & 0 & 0 \\ a_{21} & a_{22} & 0 & 0 \\ 0 & 1 & 0 & 0 \\ v & l_n & v & 0 \end{bmatrix} \begin{bmatrix} \beta \\ r \\ \Delta\varphi \\ y \end{bmatrix} - \begin{bmatrix} 0 \\ 0 \\ v \\ 0 \end{bmatrix} \rho_{ref} + \begin{bmatrix} b_{11} \\ b_{21} \\ 0 \\ 0 \end{bmatrix} \begin{bmatrix} \delta_f \end{bmatrix} \tag{23}$$

$$a_{11} = -(c_r + c_f)/mv \qquad a_{12} = -1 + \frac{c_r l_r - c_f l_f}{mv^2}$$
$$a_{21} = (c_r l_r - c_f l_f)/J \qquad a_{21} = \frac{c_r l_r - c_f l_f}{J}$$
$$a_{22} = -(c_r l_r^2 + c_f l_f^2)/Jv \qquad b_{11} = \frac{c_f}{mv}$$
$$b_{12} = c_r/mv \qquad b_{21} = c_f l_f/J \qquad b_{22} = -c_r l_r/J$$

2.2 Driver's Visual Attention Mechanism Research

The steering control problem of unmanned vehicle is a difficult nonlinear control problem, which includes the interdisciplinary theory and application of information, cognition, control, mechanical and other disciplines.

In 1994, Land and Horwood studied the human driver's driving habit while driving on a curved situation [13].The result turned out that driver's visual range was limited in an extremely small range (about 1 °around human horizontal visual height).

Driver's visual range mainly included "far"(10-20 meters from the front of the vehicle) and "near"(6-8 meters from the front of the vehicle):

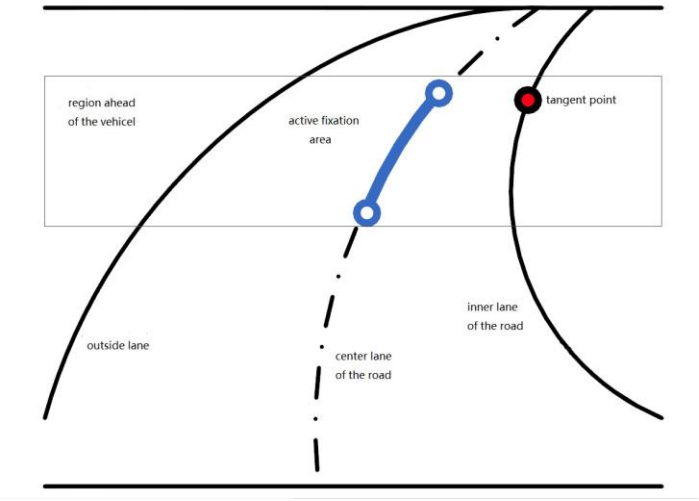

Figure 2.5: Driver Steering Fixation Area

As shown in Figure 2.5, when only distant range is visible, the experimental deviator curvature is regarded as known and the whole driving process is relatively smooth. If the near range is the only visible area, driver's driving will be choppy and the driving track will be undulated. But the vehicle will not deviate from the center line of the road when both two regions are visible. With further research, researchers found that driver would stare for a while at the point of tangency [14]. Meanwhile, the tangent area is chosen to forecast the curvature without knowing the distance from the vehicle to the tangent area.

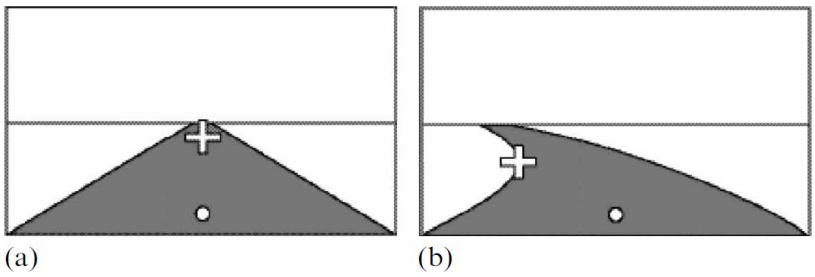

Figure 2.6: Two Points (Near and Far) Mechanism [10]

After lots of researches, Salvucci and Gray [10] deemed that driver's fixation point had multiple situations. Driver's fixation area is on the tangent point of the inner side of the track when steering as in Figure 2.6 (a); the fixation point is the vanishing point when driving on the straight road, as showed in 2.6 (b); the fixation point is the back of the front vehicle when another vehicle appears in the front.

2.3 Road Reference System

According to the methods and the theories researched above, the visual information used by drivers include far and near regions. Further driving behavior experiments can prove this viewpoint and help figure out that information from the far point makes steering control more stable and near region helps vehicle to move closer to center lane.

To compute the far and near angles, the car model in this research includes an adapted measurement equation based on the vehicle state vector and the road curvature and only takes the front steering angle into consideration as input. It's worth mentioning that some earlier research which focuses on the steering maneuver also try to reveal the connection between the two angles and highway circumstances.

However, there are more or less flaws in existing geometric relationship diagrams and calculation methods. Typically, I. Rano mistakenly regards relative yaw angle as a negative component when computing the near angle [11].Actually, the relative yaw angel is the differential angle of the centerline of the vehicle and the tangent connection path. It can be either positive or negative, based on the specific vehicle heading

direction. In addition, the relative yaw angle is not a measured value and needs to be achieved. Nevertheless, his analysis is incorrect with respect to the angle from car heading line to the R line (see the figure below) as right angle [15]. This inaccuracy will significantly influence the experimental outcome. Thus, a precise equation set is needed if we want to obtain a more accurate controller based on this measurement data.

The relationship between the two angles and road parameters is presented as:

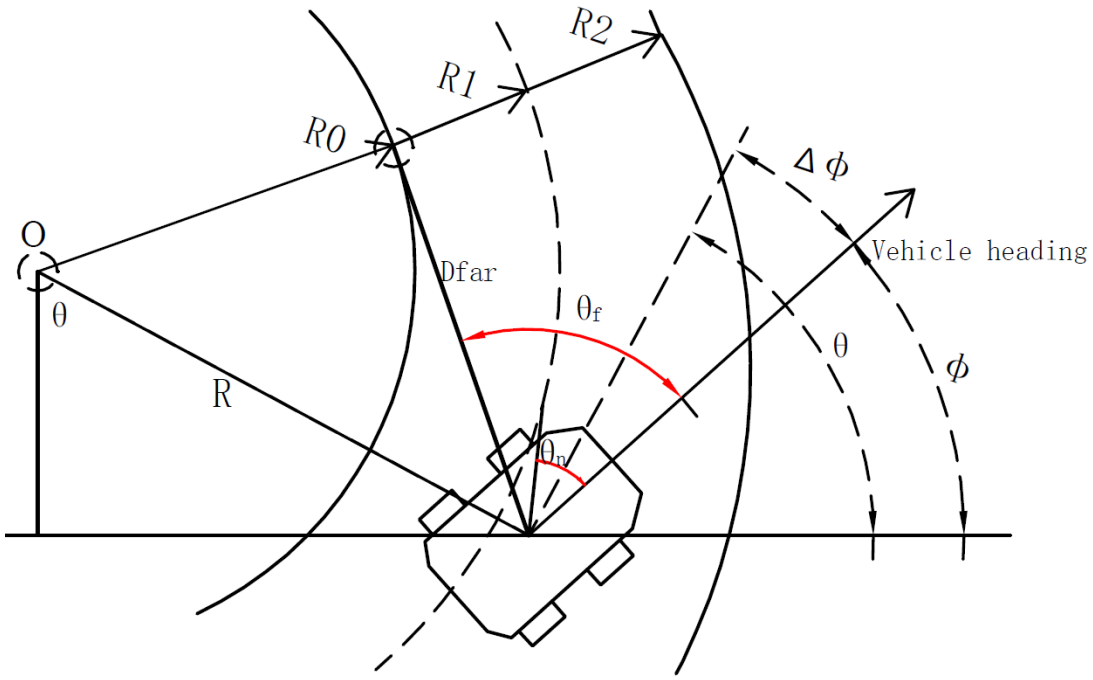

Figure 2.7: The Geometric Relationship between Vehicle and Upcoming Road

In Figure 2.7, φ is the measured yaw angle, θ is the angle between the centerline of the vehicle and the tangent path. Basing on geometrical relationships:

$$\theta = \arccos\frac{O_y - y_1}{R} \tag{24}$$

$$\Delta\varphi = \arccos\frac{O_y - y_1}{R} - \varphi \tag{25}$$

Then we can compute the near and far angles:

$$\theta_n = \arcsin\frac{y}{l_n} + \arccos\frac{O_y - y_1}{R} - \varphi \tag{26}$$

$$\theta_f = \frac{\pi}{2} - \arcsin\frac{R_0}{R} + \arccos\frac{O_y - y_1}{R} - \varphi \tag{27}$$

After linearization, the equations of these two angles are shown as

$$\theta_{\mathrm{n}} = \frac{1}{l_{\mathrm{n}}} y_l + \Delta\varphi \tag{28}$$

$$\theta_f = \frac{1}{R + y_l} D_{far} \approx \frac{D_{far}}{R} + \Delta\varphi = \frac{D_{far}}{v}\gamma + \Delta\varphi \tag{29}$$

Thus, the output matric can be achieved from the above two equations:

$$\begin{bmatrix} \theta_n \\ \theta_f \end{bmatrix} = \begin{bmatrix} 0 & 0 & 1 & \frac{1}{D_n} \\ 0 & \frac{D_{far}}{v} & 1 & 0 \end{bmatrix} \begin{bmatrix} \beta \\ r \\ \Delta\varphi \\ y \end{bmatrix} \tag{30}$$

To sum up, the complete vehicle-road model is stated as:

$$\begin{bmatrix} \dot{\beta} \\ \dot{r} \\ \Delta\dot{\varphi} \\ \dot{y} \end{bmatrix} = \begin{bmatrix} a_{11} & a_{12} & 0 & 0 \\ a_{21} & a_{22} & 0 & 0 \\ 0 & 1 & 0 & 0 \\ v & l_n & v & 0 \end{bmatrix} \begin{bmatrix} \beta \\ r \\ \Delta\varphi \\ y \end{bmatrix} - \begin{bmatrix} 0 \\ 0 \\ v \\ 0 \end{bmatrix} \rho_{ref} + \begin{bmatrix} b_{11} \\ b_{21} \\ 0 \\ 0 \end{bmatrix} [\delta_f] \tag{31}$$

$$\begin{bmatrix} \theta_n \\ \theta_f \end{bmatrix} = \begin{bmatrix} 0 & 0 & 1 & \frac{1}{D_n} \\ 0 & \frac{D_{far}}{v} & -1 & 0 \end{bmatrix} \begin{bmatrix} \beta \\ r \\ \Delta\varphi \\ y \end{bmatrix}$$

$a_{11} = -(c_r + c_f)/mv$ $\quad a_{12} = -1 + \frac{c_r l_r - c_f l_f}{mv^2}$

$a_{21} = (c_r l_r - c_f l_f)/J$ $\quad a_{21} = \frac{c_r l_r - c_f l_f}{J}$

$a_{22} = -(c_r l_r^2 + c_f l_f^2)/Jv$ $\quad b_{11} = \frac{c_f}{mv}$

$b_{12} = c_r/mv$ $\quad b_{21} = c_f l_f/J$ $\quad b_{22} = -c_r l_r/J$

2.4 Simulation Experiment Design

With the intention of obtaining the real human driver's data, simulation is conducted at the Robotics, Control, and Automation Laboratory of Texas A&M University. Co-simulation platform is established using dSpace and SIMULINK and equipped with a pedal console and a steering wheel which also can provide driver a feedback force. Meanwhile, a screen can display the simulative driving scene.

Figure 2.8: Screenshot of DSpace

As shown in Figure 2.8, a realistic virtual environment is projected onto the screen ahead driver including the upcoming road visual information, the velocity, the speed of engine and the recorded time.

The simulation software, dSpace [16] run on the corresponding workstation. The experimental parameters like vehicle mass, front and rear cornering stiffness value used in the dSpace are shown in Table 2.2. The experimental circumstance contains traffic flow, traffic signal lamp, constructions and plants. The assignments of these features can

be set up in the simulated platform before the experiment. On the other hand, drivers are allowed to change lanes or overtake other vehicles.

m	I_z	I_f	I_r	C_r	C_f	l_n
1890 kg	2400 kg m ²	1.185 m	1.106 m	97539.1(N/°)	76637.8(N/°)	7.5 m

Table 2.2 Vehicle Model Parameters in DSpace [16]

In this research, the main goal is to imitate the human driver's behavior in highway driving. To sample various habits, a standard road track for simulation is needed. The path for driving test contains a fourteen kilometers with bends of various radii can allow experimenters drive in realistic driving conditions and environments such as Figure 2.9 shown. Referring to [17], the minimum horizontal curve radius should be 620m. Thus, the test track consisting of two standard four meters wide lane is designed to contain twenty three sections including five left and five right curves whose curvatures are vary from 620m to 890m. This can help us record drivers' reaction when they face rather sharp curves or light bends. For letting the drivers keep the vehicle within the boundary of the track, bends are separated by four hundred meters long straight road. Three subjects finished the driving task. They are requested to keep the vehicle stable and moving smoothly. However, attempting to drive the vehicle in centerline is not mandatory. To obtain the more believable data, each one of them is allowed to take curves freely if they feel comfortable and easy. The one way ride took about eight minutes. During that time, it is allowed to talk to each other instead of just focusing on the simulation task. This

measure makes the results more authentic and avoids drivers' boring feeling.

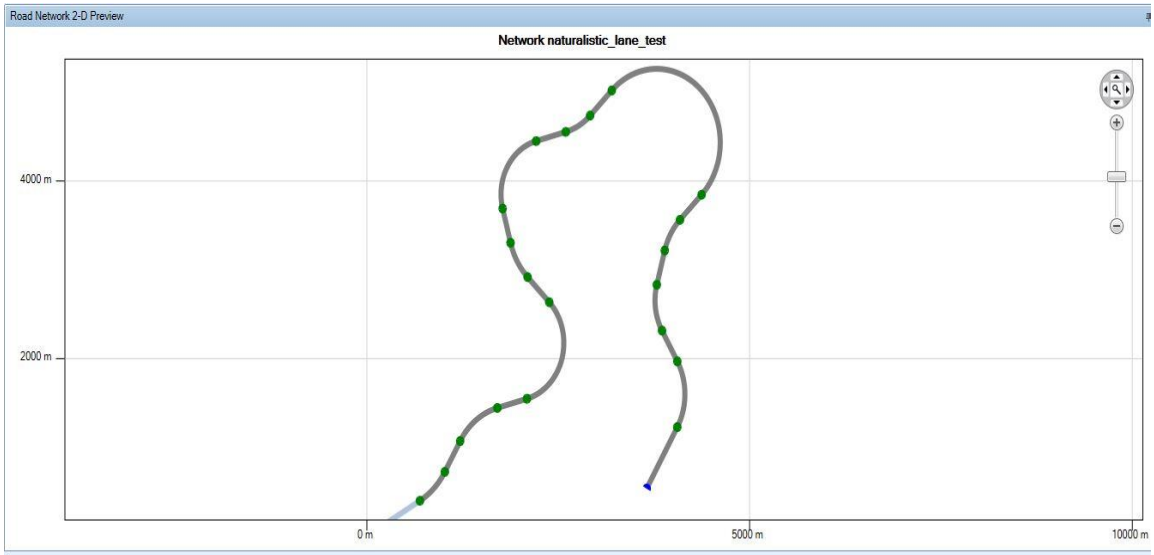

Road Network

Name	Position X [m]	Position Y [m]	Angle [°]
Type: Road			
Road 1	0.00 m	0.00 m	30.00 m
Road 10	1,773.15 m	3,690.65 m	105.00 m
Road 11	2,211.56 m	4,449.99 m	15.00 m
Road 12	2,597.93 m	4,553.52 m	15.00 m
Road 13	2,916.21 m	4,737.28 m	45.00 m
Road 14	3,199.05 m	5,020.13 m	45.00 m
Road 15	4,372.85 m	3,846.33 m	-135.00 m
Road 16	4,090.01 m	3,563.49 m	-135.00 m
Road 17	3,890.72 m	3,218.30 m	-105.00 m
Road 18	3,787.19 m	2,831.93 m	-105.00 m

Figure 2.9: Test Track in DSpace

CHAPTER III

ANALYSIS OF DRIVER BEHAVIOR

Recent studies indicate that incessant monitoring and intelligent evaluation of driving behavior and status of a driver can help to discover potential operating mistakes and hence, to avoid traffic accident; meanwhile, such monitoring and evaluation can improve traffic efficiency by alerting driver to take more appropriate driving actions to speed up [18]. Furthermore, systematically analyzing abundant of different driving behaviors can also help related departments to enact reasonable traffic laws [19].

According to the survey [20], the majority of highway speed limits range from 65 mph to 75 mph, which were converted to kmh in this study that is 104.6km/h to 120.7 km/h. All driving data acquired in this study is recorded within this speed limits range. The details of the test track are given below:

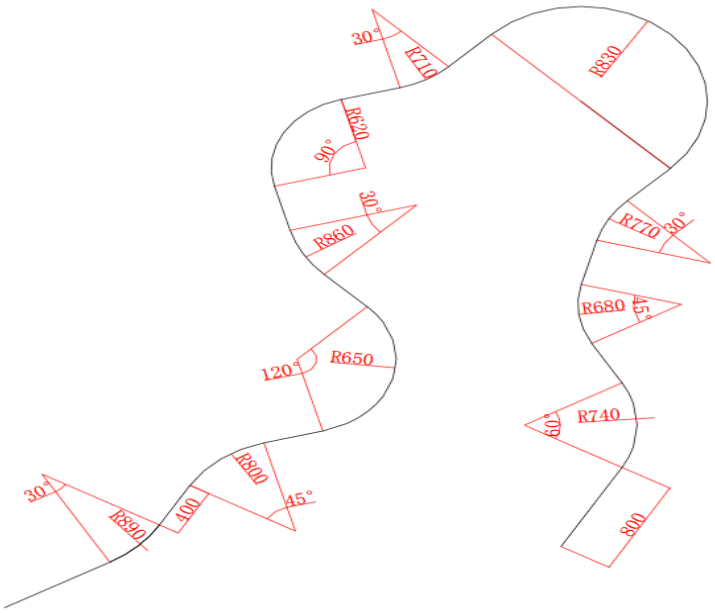

Figure 3.1: Test Track Details

The overall duration of the experiment is about eight minutes. In order to reduce the interference of other factors and simplify the analysis on the driver's driving behavior, all distractions such as vehicles, buildings or trees in experimental environment has been removed from this study. Specifically, as shown in Figure 3.2, during the driving period, the co-simulation platform recorded driving data simultaneously at the frequency of 100 HZ. All the data was recorded in real-time including the steering wheel angle, vehicle's coordinate, referring road coordinate, relative yaw angle, the steering feedback torque, and the yaw rate. These parameters were employed to calculate two inputs (near and far angle), which will adapted by the controller to imitate human driving habit.

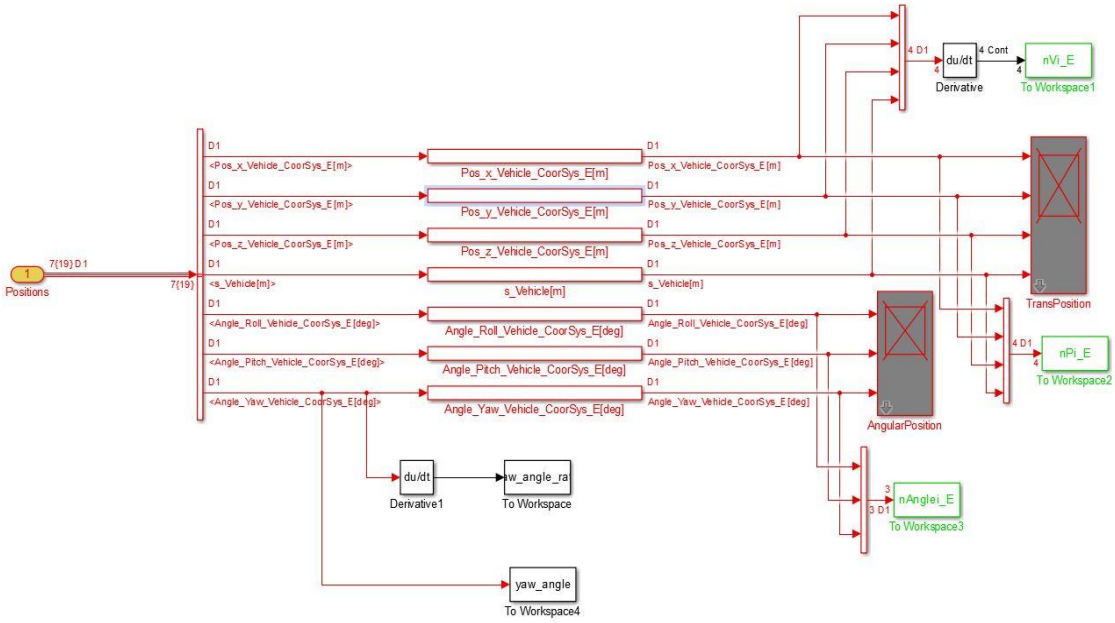

Figure 3.2: Data Recorded in DSpace

Three drivers fulfilled the driving task, which included one female and two males. The average age among them was 25 years old. On average, they received their driver licenses around 20 years-old and drove 13560 miles per year, including 6760 miles

on highways. In this study, the six sets of samples including authentic human driver behavior is recorded in Table 3.1

v \ driver	A	B	C
65 mile/h	Track 11	Track 12	Track 13
75 mile/h	Track 21	Track 22	Track 23

Table 3.1 Selected Data

3.1 Driving Strategy

Based on the measured real-time vehicle and reference road positions, three tracks recorded at 75mph plotted in Figure 3.3. In order to analyze the driving habits of three subjects quantitatively, one straight path and one curve with a red circle are chosen for driving strategy analysis.

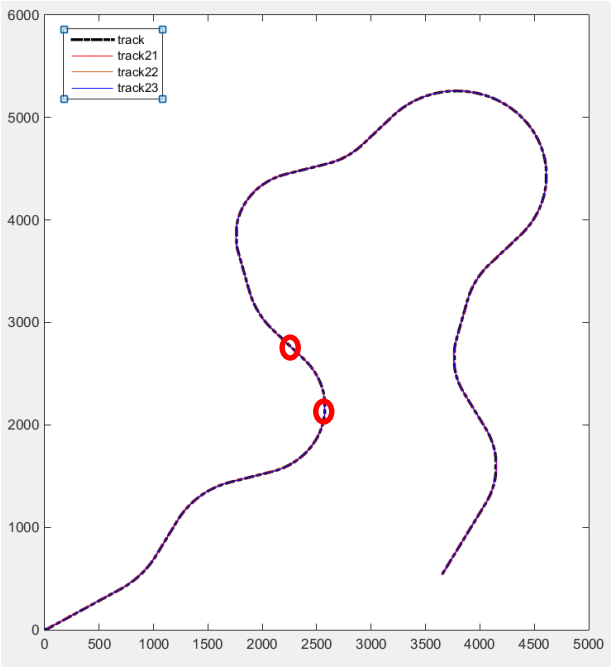

Figure 3.3: Recorded Track

If viewed as a whole, all three tracks almost match the original path. Hence, during the experiment, the driving behavior of three drivers are all appropriate, the measured data is meaningful and credible.

On the straight path circumstance as Figure 3.4 shown, the differences between these three tracks and the center lane of the road is not significant, which means drivers are always inclined to avoid the car getting too close to the both side road edge.

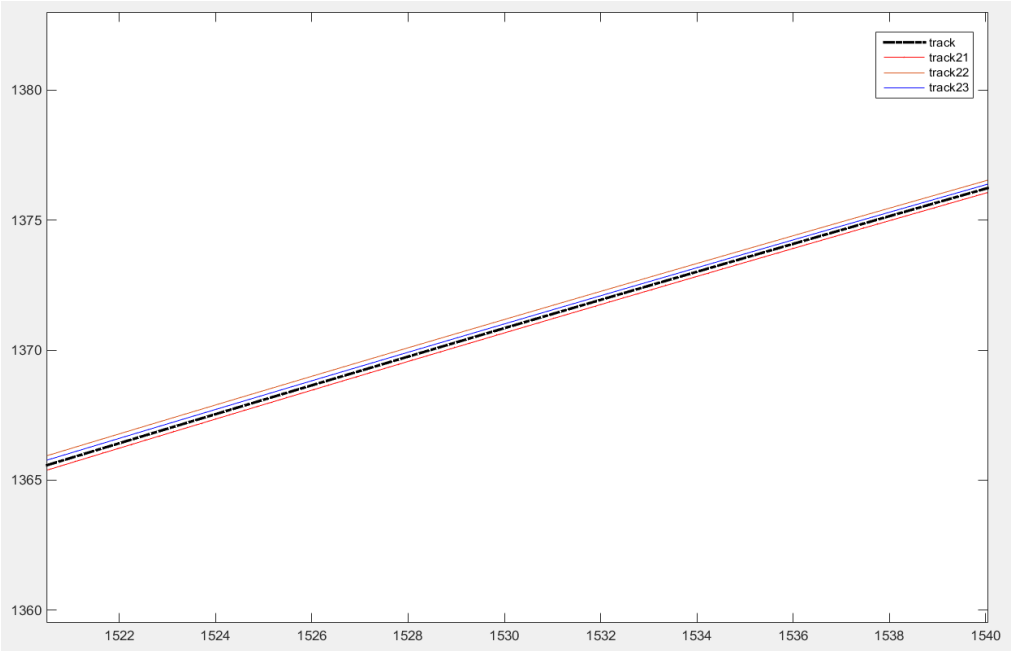

Figure 3.4: Straight Lane Comparison

The results are consistent with the research achievement from Odenheimer, Germaine L [22] that the majority of experienced driver primarily consider safety. Therefore, the problem of how the driver take a curve should be the first thing we take into consideration.

To judge whether the driver is pursuing speed and saving time, the racing line in Figure 3.5 is an important concept which means the path that should be chosen to

minimize the duration of passing curve operation. The fastest line while analyzing a single bend is the one on which the passing time can be reduced and the average velocity through the bend can be maximized. Driver can minimize the driving distance if the path with the smallest radius is chose [24].

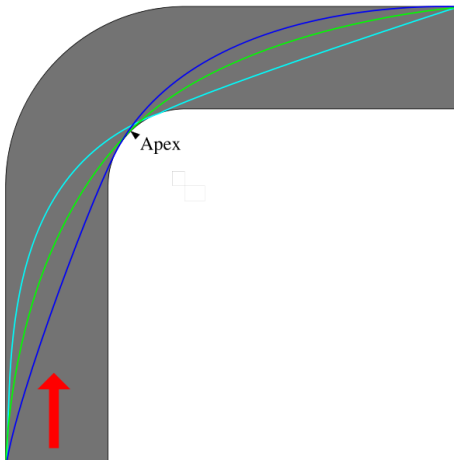

Figure 3.5: The Racing Line [23]

In contrast with straight condition, three drivers showed distinct difference of their steering maneuver. As shown in graph, although they all reveal the tendency of cutting corners, there is significant diversity on details of their driving behavior such as in Figure 3.6.

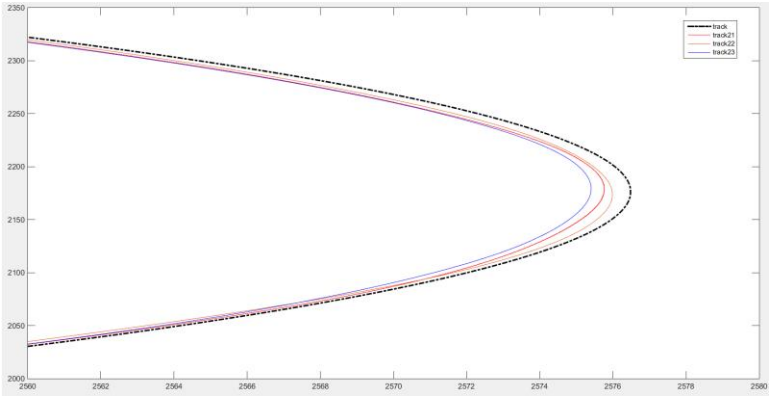

Figure 3.6: Bend Comparison

This study mainly investigate three diverse driving styles：By trying to stay in the most reasonable site of the route and keeping a moderate interval to the tangent point of the bend that is presented effective curve taking, which an experienced car user always conducts, the first subject balanced speed and safety. The second driver attempted to stay closer to the center lane, which is considered as a typical cautious way of steering with minimum lateral deviation error. It is worth noting that the driving path of this driver is not as smooth as other two drivers. The turning radius during second half is larger than which in first half, which is due to fact that the second subject was less driving experience. In addition, the absence of the ability to get the precise perception of the road curvature may be the second reason of this phenomenon. The driving style of the third driver seems the most aggressive one. He cut bends and tried to follow the shortest path and make the vehicle get closer to the apex of the curve.

3.2 Analysis of Steering

The track comparison can only reveal the driving behavior in a rough manner. To learn the correlation between the controller parameters and the real driving performance more specifically, steering angle and lateral offset as well as near and far angle are chose as primary variables to analyze.

To take the curve mentioned on last section, three drivers produced different response patterns. As Figure 3.7 shows, three steering angles all fluctuate within a certain range. However, the frequency of adjusting the angle and the amplitude are diverse. Based on JMP software [25], we can determine the sample mean, median, and standard deviation

of each data set.

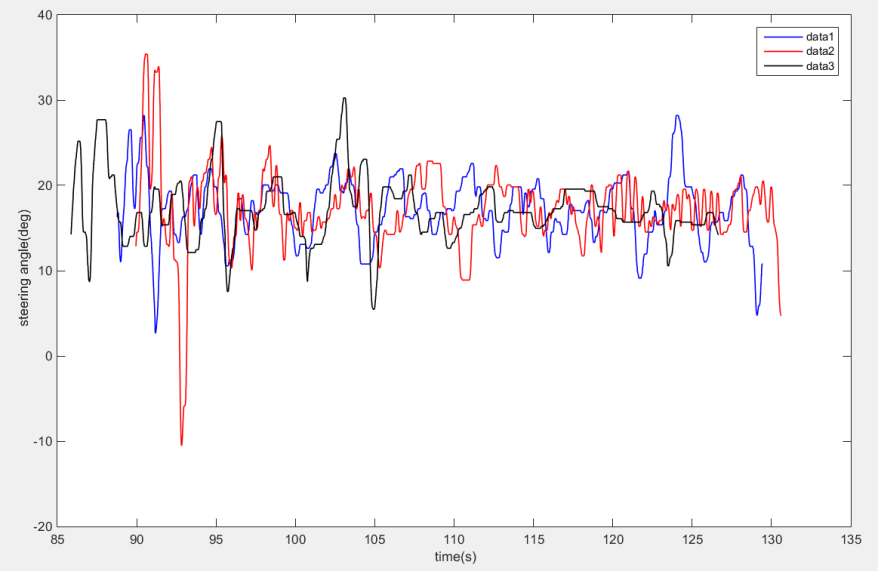

Figure 3.7: Steering Angle of Three Drivers

The same analytical methods will also be applied to other parameters. This information will play an essential role in the quantitative analysis of driving behavior. As the software interface shows in Figure 3.8, the distribution of each data set during the taking turve period and the values mentioned above are exhibited clearly.

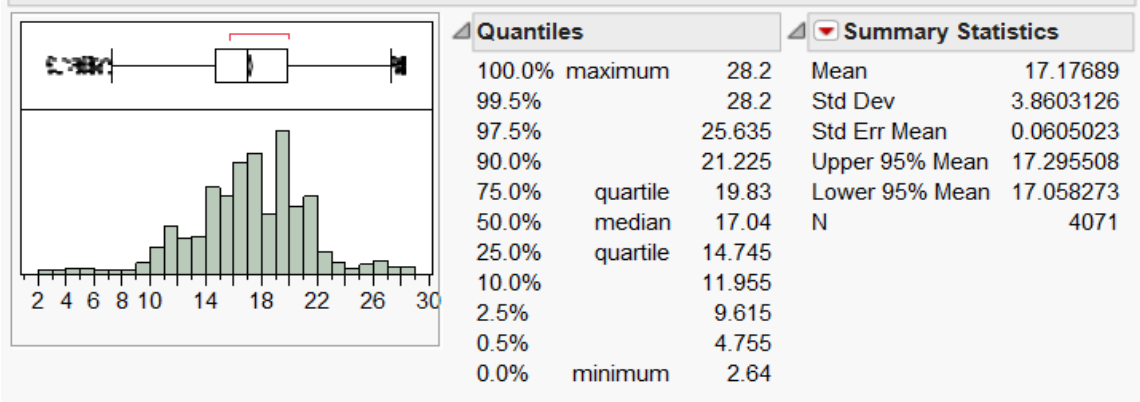

Figure 3.8: JMP Example

By integrating the processing results, the comparison of drivers' steering angle

is presented in table 3.2.

PARAMETER / ***DRIVER***	MEAN (deg)	MEDIAN （deg）	STD DEV (deg)
1	17.18	17.04	3.86
2	17.25	17.04	4.65
3	17.23	16.82	3.72

Table 3.2: Comparison of Steering Angle

As shown in the table above, three driver's steering angles are extremely close, and fluctuate around 17.2 degree. Here, median and standard deviation should be paid attention to. Outlier is the main cause that lead to the difference in the median and mean. More outlier points exist in statistics indicated a larger variation in data. In statistics field, a point that has a rather longer distance from other observations is defined as outlier [27]. The third driver's median is only 16.82 degrees, which is significantly lower than the other two drivers'. This is because the driver chose the most radical curve route, which means the driver will spend more time on the straight path. Besides, the numbers of variations or dispersions in a set of data are used to be measured by standard deviation. Among a wide range of values, data points are going to spread out if there exists a higher standard deviation [28]. The second driver's standard deviation is 4.65 degrees, which is 30 percent higher than the other two drivers'. As known from the Figure 3.5, this is because the second driver lacks driving experience and she produced jagged steering. Consequently, the steering angle fluctuation is intense, though the driver chose the route that is close to the center lane.

3.3 Calculation of Two Angles

From Figure 2.7, Dfar and lateral offset are presented as:

$$D_{far} = \sqrt{R^2 - R_0^2} \tag{32}$$

$$y_l = |R - R_1| \tag{33}$$

After calculation, we can use excel to record each variance including Dfar and lateral offset like:

A	B	C	D	E	F	G	H	I	J	K	L	M	N	O	P
time	x1	y1		x0	y0		0x	0y		R	R0	R1		Dfar	lateral
85.86	2105.765	1548.184		2105.68	1548.475		1922.486	2176.293		654.3025	652	654		54.84307	0.302545
85.87	2106.083	1548.273		2105.997	1548.567		1922.486	2176.293		654.306	652	654		54.88446	0.306015
85.88	2106.401	1548.363		2106.314	1548.66		1922.486	2176.293		654.3095	652	654		54.9266	0.309551
85.89	2106.719	1548.452		2106.63	1548.753		1922.486	2176.293		654.3131	652	654		54.96946	0.313151
85.9	2107.036	1548.542		2106.947	1548.846		1922.486	2176.293		654.3168	652	654		55.01303	0.316813
85.91	2107.354	1548.631		2107.264	1548.939		1922.486	2176.293		654.3205	652	654		55.05729	0.320535
85.92	2107.672	1548.721		2107.58	1549.032		1922.486	2176.293		654.3243	652	654		55.1022	0.324316
85.93	2107.99	1548.811		2107.896	1549.125		1922.486	2176.293		654.3281	652	654		55.14774	0.328152
85.94	2108.307	1548.901		2108.213	1549.219		1922.486	2176.293		654.332	652	654		55.19387	0.332042
85.95	2108.625	1548.991		2108.529	1549.313		1922.486	2176.293		654.3359	652	654		55.24057	0.335983
85.96	2108.942	1549.081		2108.846	1549.407		1922.486	2176.293		654.3399	652	654		55.2878	0.339971
85.97	2109.26	1549.171		2109.162	1549.501		1922.486	2176.293		654.344	652	654		55.33551	0.344005
85.98	2109.577	1549.262		2109.478	1549.595		1922.486	2176.293		654.348	652	654		55.38369	0.34808
85.99	2109.895	1549.352		2109.794	1549.69		1922.486	2176.293		654.3522	652	654		55.43228	0.352195
86	2110.212	1549.443		2110.11	1549.784		1922.486	2176.293		654.3563	652	654		55.48125	0.356346

Table 3.3: Data Processing Example in EXCEL

Through Figure 3.9, we can observe the variation trend of far distance as:

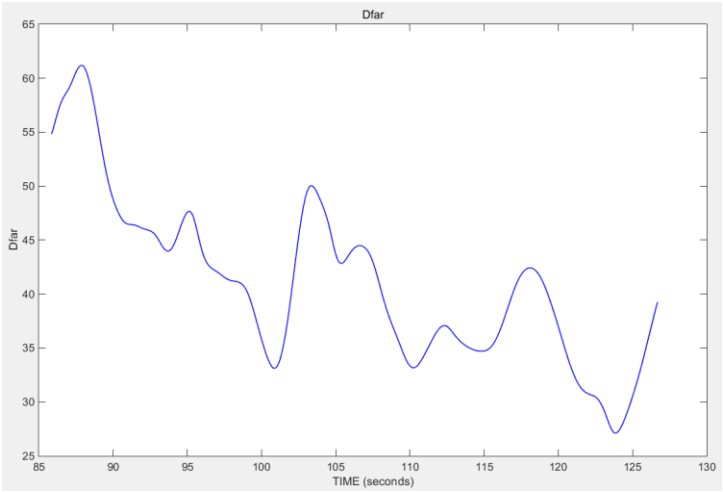

Figure 3.9: Far Distance

On curve 1, average Dfar is 41.026m and average lateral distance is 0.77m, which also proves that assuming the vehicle is always in the lane center is incorrect. Based on the nonlinear Equations (26) and (27), the near and far angle can be drawn as figure 3.10.

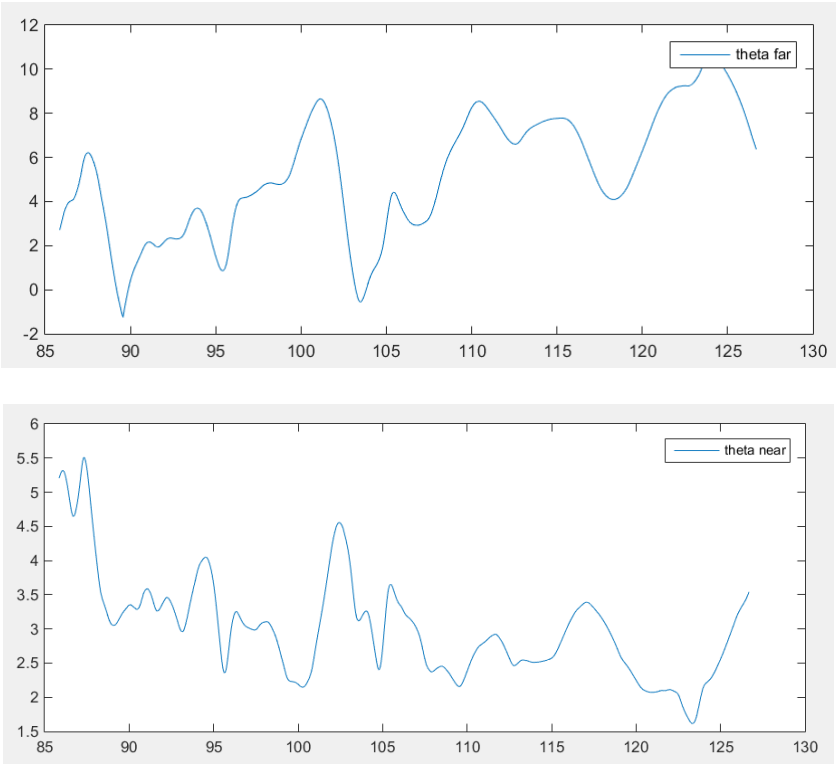

Figure 3.10: Far and Near Angle

Through this data processing method, we can achieve the variation tendency of the two angles during each curve taking period. In the next chapter, these two angles will act as input of the human-like controller system.

CHAPTER IV

SIMULATION AND RESULTS

According to the analysis of driver behavior in the previous chapter, information of the upcoming curve and the estimation of real-time vehicle location are the mainly inputs of human driver. In this naturalistic lane keeping system which relies on a two reference point control mechanism, these information are equal to near and far angles. Meanwhile, since the steering angle is the most direct element connecting the driver and the vehicle, it is regarded as the only outcome of the driver model.

Generally speaking, modeling approaches can divide into First-Principles Modeling (Model-Based) and Data-Driven Modeling as figure 4.1 [29] shows. Specifically, the model-based approach tries to directly calculate a physical quantity from already known physical laws. [30]. On the contrary, the plant model under the Data-Driven method is identified by collecting and processing real data from an existing experimental system and choosing an appropriate mathematical algorithm with which to determine a corresponding model.

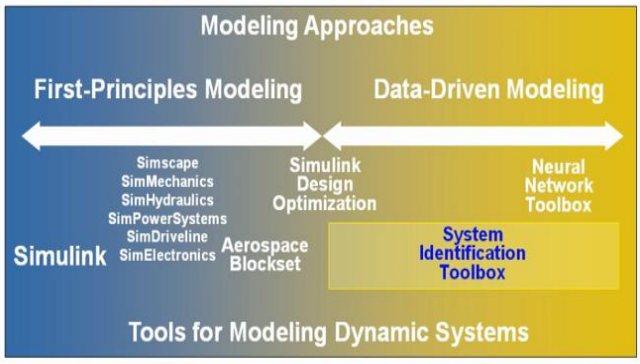

Figure 4.1: Modeling Approaches [29]

In this study, all the parameters including four variables and real-time vehicle

position are recorded by dSpace software. Thus, Data-Driven Modelling method is chosen as the ideal way to determine the driver model. To structure a completed driver-vehicle system, a driver model is designed using a close-loop proportional–integral controller first in this section. In addition, system identification tool is also widely used in data processing work. Several methodologies are being discussed and compared in the second section of this chapter.

4.1 PI Controller Identification

One of the commonly adopted control loop feedback structures among is the proportional-integral (PI) controller. The discrepancy between variables measured in the process and the desired set point can be calculated by such a controller. By adjusting controlling variable, the controller aims to reduce the error incidence over time. The mechanism of PI controller can be presented as:

$$\mathrm{u(t)} = K_p e(t) + K_i \int_0^t e(\tau) d\tau \tag{34}$$

where K_p and K_i mean the coefficients of the proportional and integral terms correspondingly. A PI controller only relies on the measurement, not on knowledge of the underlying process. Furthermore, the integral action is the important element of PI controllers since it permits PI controller to eliminate the main weakness of the P-only controller. As a result, the balance between complexity and capability enables the PI controllers the most extensively utilized algorithm [32].

In this case, consider the real-time near and far angle given in last chapter, the structure of whole system can be plotted as follows:

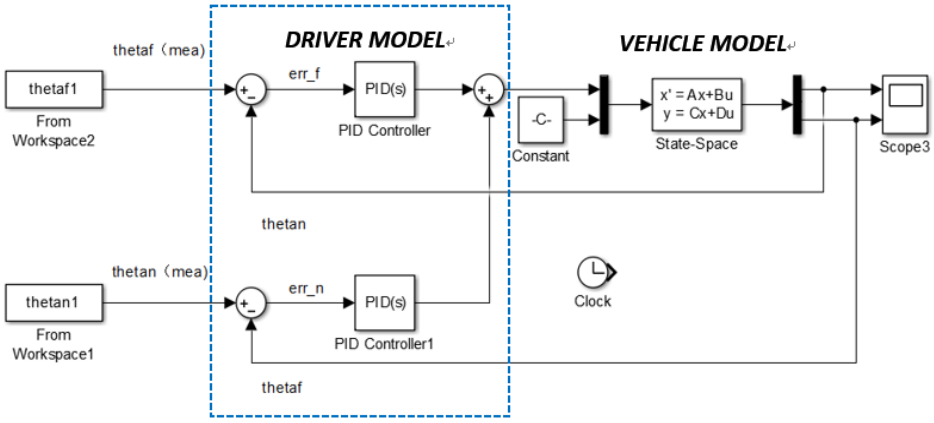

Figure 4.2: System Structure using PI Controller

The system is made up of the driver model and the vehicle model. More specifically, the near angle and the far angle are set as the measured process variables of the whole system. Through two PI controller connected with errors of two angles separately, the outputs of vehicle model can be match with the desired angles to achieve the goal of naturalistic lane keeping, which means the vehicle will move follow the track like being controlled by real person. In order to tune the two PI controllers more conveniently and directly, SIMULINK is chose as the experimental platform. The aim of the experiment is matching the simulated curve with measured curve meantime. Given that the two controllers will affect each other during the experiment, tuning four parameters of PI controllers to find an equilibrium point should be the emphasis and difficulty in this case.

For instance, the curve in Figure 3.2 is chose for model fitting and the radius of this curve is 650m. After tuning, the PI controller can accurately reflect the characteristics of the human driver#3 as the following two figures show.

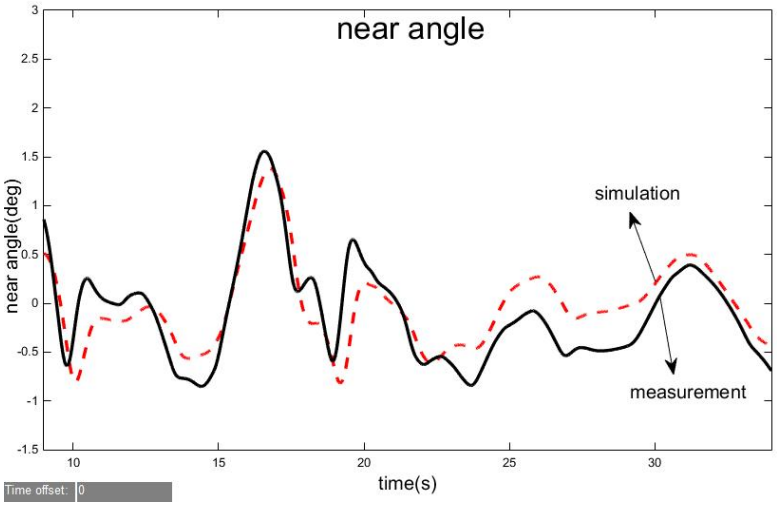

Figure 4.3: Near Angle Comparison

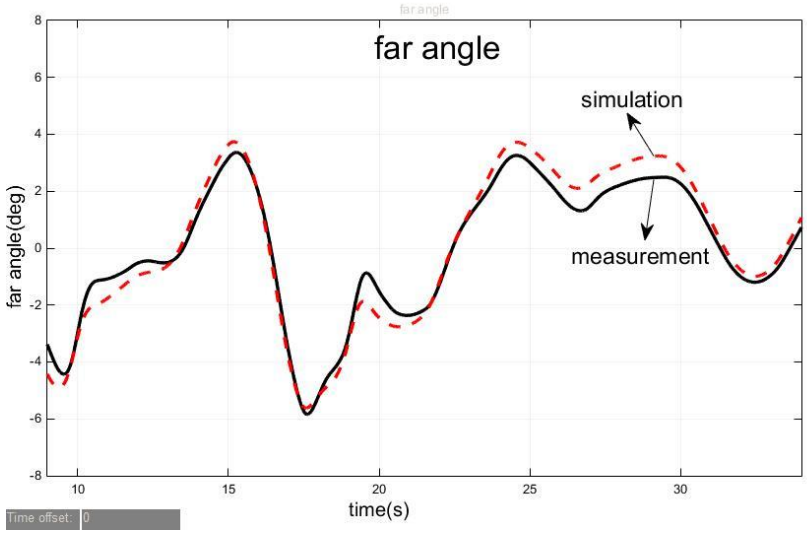

Figure 4.4: Far Angle Comparison

Via the figure above, the simulated curve basically matches with the authentic curve and the far angle's matching point is relatively higher. If quantitative analysis is going to be conducted, two fundamental conceptions should be introduced at first. L1-norm and L2 norm are two generally-used method for regularization.

L1-norm represents least absolute deviations (LAD) or least absolute errors

(LAE) [33]. The sum of the absolute differences (S) between the estimated values f(x_i) and the target value (Yi) can be minimized:

$$S = \sum_{i=1}^{n} |y_i - f(x_i)| \tag{35}$$

L2-norm is also acknowledged as least squares. The sum of the square of the differences (S) between the estimated values f(x_i) and the target value (Yi) is minimized [34]:

$$S = \sum_{i=1}^{n} (y_i - f(x_i))^2 \tag{36}$$

The identification match percentage can be calculated as:

$$\text{Macth}(\%) = \left(1 - \frac{norm(l - \hat{l})}{norm(l - l_{mean})}\right) * 100 \tag{37}$$

Where l is the measured value, $\hat{l}$ is the simulated value and l_{mean} is the mean value of l. Through calculation, two angles obtained by identification model is close to the measurement with ideal match percentage:

Norm / *Variables*	**L1-Norm**	**L2-Norm**
far angle	87.64	86.10
near angle	68.57	67.42

Table 4.1 Match Percentage of Identification Model

The match percentage test demonstrates that this type of driver model can achieve the goal of matching two angles simultaneously and accurately. Nevertheless, to check the validation of the whole system, the comparison between the measurement and the simulated values need to be done for both lateral offset and vehicle path.

Basing in the simulated value of the two angles and the geometric relationship, the lateral offset comparison of the three drivers is plotted as Figure 4.5 shows.

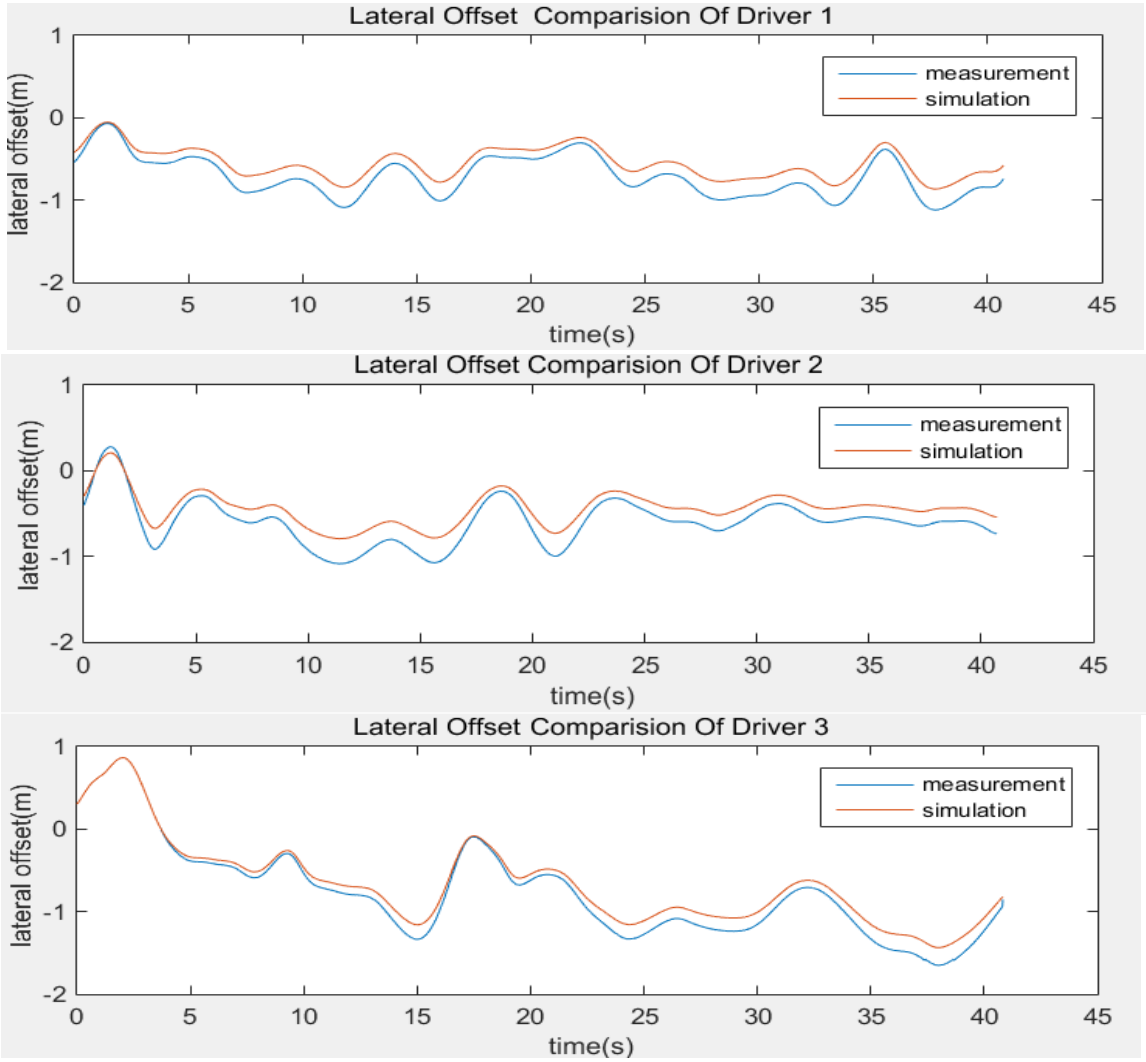

Figure 4.5: Lateral Offset Comparison

In particular, the first driver keeps on relatively moderate lateral offset from the centerline to optimize the moving path. The second driver attempt to get most close to center lane for pursuing the feeling of safety. In contrast, the value of lateral offset is the largest for the last driver among the three subjects. Most notably, driver#3 turns the steering wheel to the outside edge direction. As analysis in the last chapter shows this activity can be explained as obtaining enough space to cut the curve sharper during the process of entering the bend.

The whole course of passing a curve can be divided into three steps of entering the curve, taking the curve and existing the curve as Figure 4.6 shows.

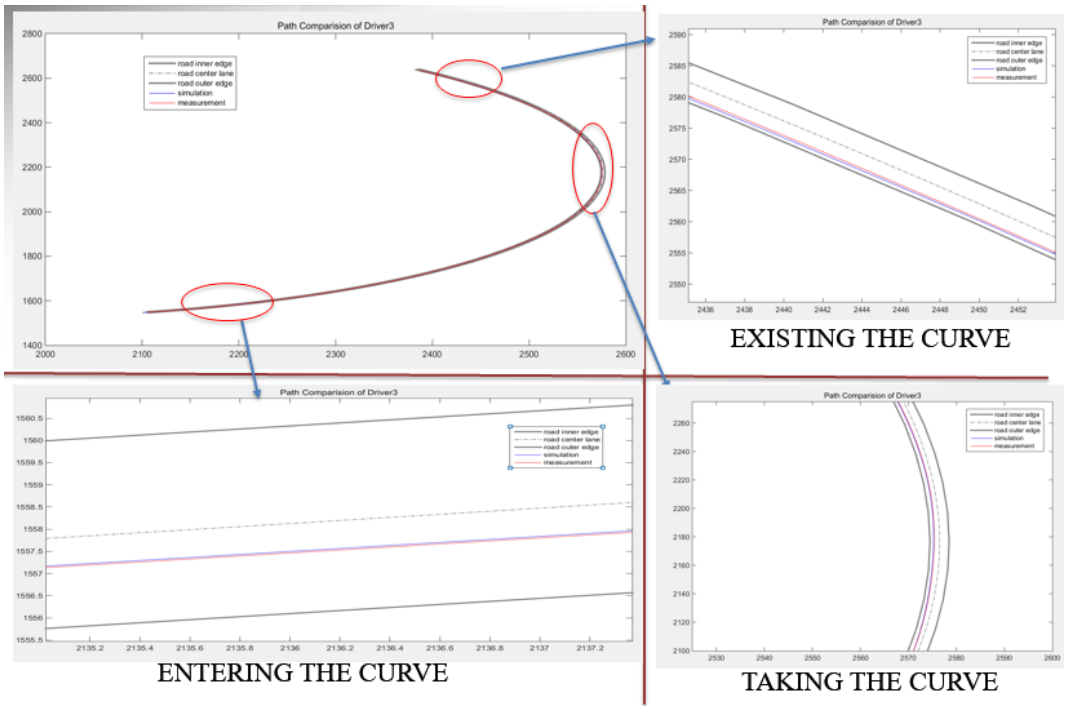

Figure 4.6: Three Steps

There are apparent differences between the drivers in entering the curve; each chooses to enter the curve on inner, center and outer lane individually.

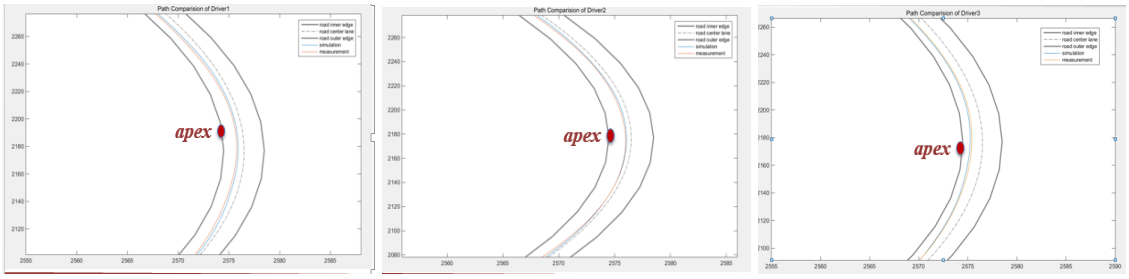

Figure 4.7: Comparison of Path on Taking Curve Step

To compare the three diverse cutting curve strategies, the apex points are added in Figure 4.7. The experimental results are consistent with the recorded data which has

been discussed in Chapter three. The first driver follows the most reasonable path, the second inexperienced drive have the longest distance to apex, and the third aggressive driver run the vehicle getting closer to apex point. Consequently, the driver-vehicle model can realize the naturalistic function of catching every driver's personalized habit.

4.2 Modelling by System Identification Toolbox

The above system based on PI control can capture human driving behavior correctly, however, there remain limitation and shortcomings. Firstly, there are some distortion problem existing in the beginning and end period of simulation. In addition, the parameters applied to the driver model need to be tuned manually. To increase the ability of driver model and save the time of parameters identification, the system identification toolbox (SIT) is introduced to provide us an alternative approach of focusing on driver model and establishing an open loop system [29].

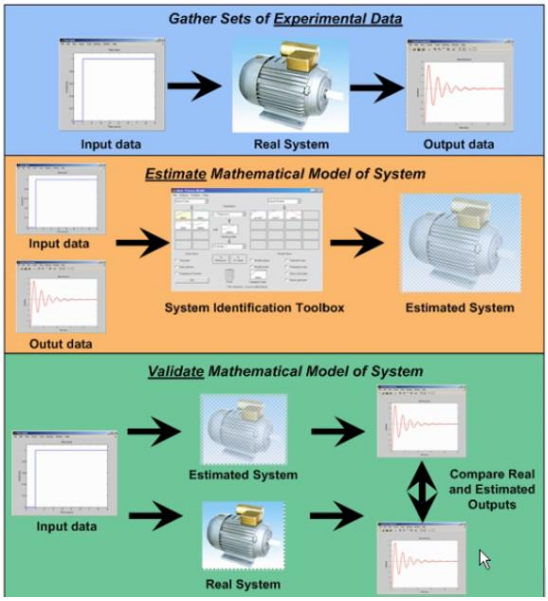

Figure 4.8 SIT Data Processing Flow [29]

Generally speaking, SIT data processing work consists of three steps:

- Collect data based on experiment
- Identify controller model

  ---determine the structure of prospective model

  ---Select a matched model
- Conduct validation work with independent experimental data

The data, which is used to estimate model, is the first section of measurement, then, use the estimated model we can obtain the result to compare it with the authentic second section. Thus, the validation problem has been considered when identifying the model. This is also the key different between the two controllers in this thesis as Figure 4.9 [29] shows.

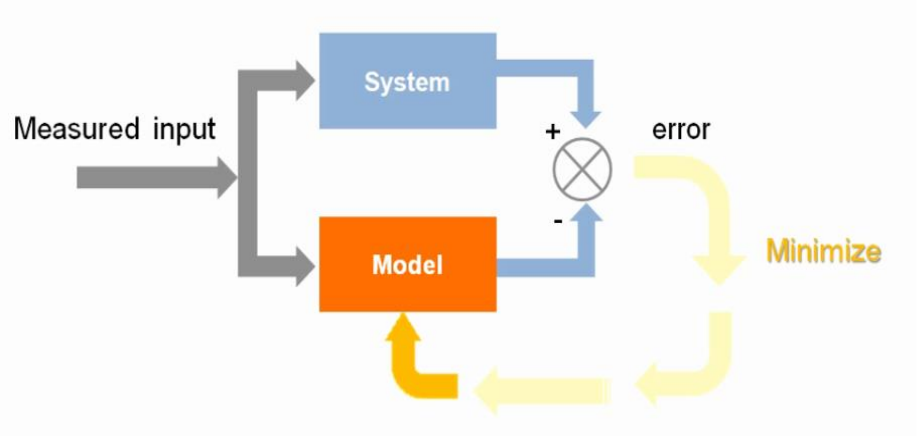

Figure 4.9 SIT Identification Mechanism [29]

In this case of open loop driver model design, it is straightforward to compare the steering angle as the output of the controller for the reason that all the data needed has been recorded by the experimental platform.

There are several different method to identify the driver model such as linear

ARMAX model, linear ARX model, Hammerstein-Wiener Model and Nonlinear Grey-box model. After comparison and taking the complexity of experimental data into consideration, the multi-input nonlinear ARX and Hammerstein-Wiener models is chose as the algorithm used in this driver identification work as Figure 4.9 shown. The inputs of the open-loop system are the measurements of near and far angle and the output of driver model is steering angle. It is noteworthy that the output is different from the PI controller output mentioned above, in that case, the driver control generate front wheel steering angle.

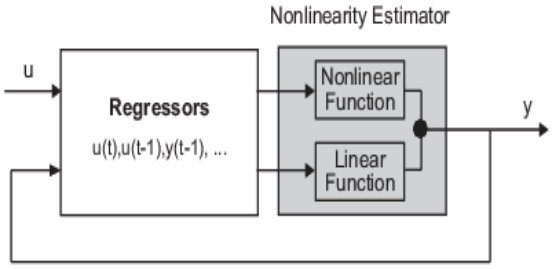

Figure 4.10 Nonlinear ARX Identification [29]

The changing of steering angle is the parameter which give the driver most intuitive feeling in both visual and auditory senses. Hence, the steering angle is chose as the value under comparison in Figure 4.10 [29].

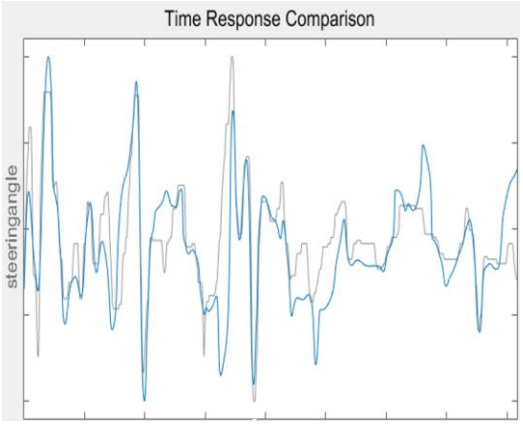

Figure 4.11 Steering Angle Comparison

In this figure, the grey line is the measured steering wheel angle and the blue line is the simulated value. These two curve almost match with each other that reflects the nonlinear ARX model is applicative in this open loop driver model.

CHAPTER V

CONCLUSION AND OUTLOOK

5.1 Conclusion

Focusing on the driver model of intelligent vehicle steering control, this thesis studied how human drivers obtain surrounding driving circumference, how they learn and master vehicle's dynamic characteristics while driving. All the details are presented below:

(1) By summarizing and analyzing previous researches, the thesis established the preview vehicle-road reference model which based on near and far points mechanism and gained the transfer function about preview information and expected hanging angle.

(2) With the combination of designed internal robust tracking steering controller and preview model which integrated the vehicle lateral dynamic characteristics and derivers' physical limitations, a simulation experiment was conducted, which verified the correctness of the whole system implemented with driver model and vehicle model.

(3) Designed nonlinear steering driver model can effectively correct steering wheel angel by minimizing the error between different outputs of real model and simulated model, which also can be applied on the vehicle's parameter changing or uncertainty in existing conditions.

5.2 Outlook

The thesis established the model about visual information input that bears human driver's characteristics and driver's self-adaptive behavior characteristics. These parts, however, fulfill only parts on imitating human driver's characteristics, and there are

still many sections left behind. Further researches about how drivers make reasonable steering decisions by visual information or about the implementation process (arms' neuromuscular system model) are needed.

In fact, the imitation circumstance in the article is a driver-vehicle-route closed-loop imitation system. Besides the visual feedback (location, obstacle, etc.,) given by the road, there is also tactile sensation feedback signal during real driving. To achieve automatic driving, it is necessary to take the influence brought by real conditions into account and such consideration can make the automatic driving more steady, comfortable, safe, and practical.

REFERENCES

[1] Tefft, B. C. (2014). Prevalence of motor vehicle crashes involving drowsy drivers, United States, 2009–2013. *Rep. Prepared for the American Automobile Association (AAA) Foundation for Traffic Safety, Washington, DC*.

[2] Lane keeping system. Retrieved from *http://owner.ford.com/how-tos/vehicle-features/safety/lane-keeping-system.html*

[3] Pohl, J., Birk, W., & Westervall, L. (2007). A driver-distraction-based lane-keeping assistance system. *Proceedings of the Institution of Mechanical Engineers, Part I: Journal of Systems and Control Engineering*, *221*(4), 541-552.

[4] Kondo, M. (1953). Directional stability (when steering is added). *Journal of the Society of Automotive Engineers of Japan (JSAE)*, *7*(5-6), 9.

[5] Donges, E. (1978). A two-level model of driver steering behavior. *Human Factors: The Journal of the Human Factors and Ergonomics Society*, *20*(6), 691-707.

[6] Zeyada, Y., El-Beheiry, E., El-Arabi, M., & Karnopp, D. (2000). Driver modeling using fuzzy logic controls for human-in-the-loop vehicle simulations. *Current Advances in Mechanical Design and Production VII*.

[7] Hessburg, T., & Tomizuka, M. (1994). Fuzzy logic control for lateral vehicle guidance. *Control Systems, IEEE*, *14*(4), 55-63.

[8] MacAdam, C. C., & Johnson, G. E. (1996). Application of elementary neural networks and preview sensors for representing driver steering control behaviour. *Vehicle System Dynamics*, *25*(1), 3-30.

[9] Kraiss, K. P., & Kuttelwesch, H. (1993, May). Identification and application of neural operator models in a car driving situation. In *IFAC Symposia Series* (Vol. 5, pp. 121-126).

[10] Salvucci, D. D., & Gray, R. (2004). A two-point visual control model of steering. *Perception-London*, *33*(10), 1233-1248.

[11] Rano, I., Edelbrunner, H., & Schoner, G. (2013, June). Naturalistic lane-keeping based on human driver data. In *Intelligent Vehicles Symposium (IV), 2013 IEEE* (pp. 340-345). IEEE.

[12] Ackermann, J. (2012). *Robust control: Systems with uncertain physical parameters*. Springer Science & Business Media.

[13] Land, M., & Horwood, J. (1995). Which parts of the road guide steering? *Nature*, *377*(6547), 339-340.

[14] Salvucci, D. D. (2006). Modeling driver behavior in a cognitive architecture. *Human Factors: The Journal of the Human Factors and Ergonomics Society*, *48*(2), 362-380.

[15] Sentouh, C., Chevrel, P., Mars, F., & Claveau, F. (2009, October). A sensorimotor driver model for steering control. In *Systems, Man and Cybernetics, 2009. SMC 2009. IEEE International Conference on* (pp. 2462-2467). IEEE.

[16] DSpace Software. Retrieved from *https://en.wikipedia.org/wiki/DSpace*

[17] KILINÇ, A. S., & Baybura, T. (2012). Determination of minimum horizontal curve radius used in the design of transportation structures, depending on the limit value of comfort criterion lateral jerk. *TS06G-Engineering Surveying, Machine Control and Guidance, Rome, Italy*.

[18] Wang, W., Sun, F., Cao, Q., & LIU, S. (2001). Driving behavior theory and its application in road traffic system.

[19] Straus, S. H. (2002). “New, Improved, Comprehensive, and Automated Driver's License Test and Vision Screening System. *Journal of Experimental Psychology, 11*, 122-132.

[20] Haglund, M., & Aberg, L. (2000). Speed choice in relation to speed limit and influences from other drivers. *Transportation Research Part F: Traffic Psychology and Behaviour*, *3*(1), 39-51.

[21] Li, L., Wang, F. Y., & Zhang, Y. (2007). Research and developments of intelligent driving behavior analysis. *Acta Automatica Sinica*, *33*(10), 1014.

[22] Odenheimer, G. L., Beaudet, M., Jette, A. M., Albert, M. S., Grande, L., & Minaker, K. L. (1994). Performance-based driving evaluation of the elderly driver: safety, reliability, and validity. *Journal of Gerontology*, *49*(4), M153-M159.

[23] Racing line. Retrieve from https://en.wikipedia.org/wiki/Racing_line

[24] Beckman, B., & Club, N. B. R. (1991). The Physics of Racing, Part 5: Introduction to the Racing Line. *Online] http://www. esbconsult. com. au/ogden/locust/phors/phors05. htm*.

[25] Goupy, J., & Creighton, L. (2007). *Introduction to design of experiments with JMP examples*. SAS Publishing.

[26] Bamnett, V., & Lewis, T. (1994). Outliers in statistical data

[27] Grubbs, F. E. (1969). Procedures for detecting outlying observations in samples. *Technometrics*, *11*(1), 1-21.

[28] Bland, J. M., & Altman, D. G. (1996). Statistics notes: measurement error.*Bmj*, *313*(7059), 744.

[29] Ljung, L. (1995). *System identification toolbox: User's guide*. MathWorks Incorporated.

[30] Pantelides, C. C., & Renfro, J. G. (2013). The online use of first-principles models in process operations: Review, current status and future needs.*Computers & Chemical Engineering*, *51*, 136-148.

[31] O'Dwyer, A. (2009). *Handbook of PI and PID controller tuning rules* (Vol. 57). London: Imperial College Press.

[32] Ho, W. K., Hang, C. C., & Cao, L. S. (1992, May). Tuning of PI controllers based on gain and phase margin specifications. In *Industrial Electronics, 1992. Proceedings of the IEEE International Symposium on* (pp. 879-882). IEEE.

[33] Donoho, D. L. (2006). For most large underdetermined systems of linear equations the minimal ℓ1 - norm solution is also the sparsest solution. *Communications on pure and applied mathematics*, *59*(6), 797-829.

[34] Baraniuk, R. G. (2007). Compressive sensing. *IEEE signal processing magazine*, *24*(4).